Performance Analysis of the Photon-Counting LIDAR Based on the Statistical Property

Jun Dai[1(✉)], Shaohui Li[1], Fei Gao[2], Haiyi Cao[1], Gaofeng Guo[1], Xigang Liu[1], and Qianying Wang[1]

[1] Institute of Remote Sensing Satellite, China Academy of Space Technology, Beijing, China
`haojundj@163.co`
[2] DFH Satellite Co., Ltd., Beijing, China

Abstract. Combined with Lidar equation and single photon detection probability theory, the photon-counting Lidar performance indexes under different parameters are studied. The analysis shows that when the surface reflectance is relatively low and the slope is gentle, higher detection probability can be caculated by increasing the grid size of the ground surface. In the case of 1 MHz noise rate, when the frame threshold of the photon counts is 3pe, the detection probability of 99.78% can be achieved. In the case of 10 MHz noise rate, when the frame threshold of the photon counts is 7pe, detection probability of 97.7% can be achieved. Finally, a feasible parameter suggestion of photon-counting spaceborne Lidar is given.

Keywords: Photon counting · LIDAR · Statistical property

1 Introduction

As a kind of active remote sensing technology, spaceborne Lidar has been widely recognized by the space industry and is developing rapidly [1]. Since the 1990s, the satellites with ranging Lidar have made great progress in a series of space science applications, especially in deep space exploration and earth observation [2–4]. Threshold method or full waveform method widely used in these ranging Lidar to measure the distance between the satellite and the planet.

Photon detection Lidar is a new method based on probability and statistics to accurately measure the distance. Due to the requirement for laser pulse of photon-counting is three orders of magnitude lower than that of linear detecting system, it makes spaceborne Lidar with hundreds beams or even thousands beams possible. ICESat-2 satellite is a global earth observation satellite based on single photon detection system [5]. It was the next follow-on environmental mission of ICESat-1 which was launched on September 15, 2018. The Advanced Topographic Laser Altimetry System (ATLAS) is the sole instrument of ICESAT-2 has six beams and a repetition rate of 10 kHz, which makes 0.7 m along-track spacing of <17 m diameter footprints [6].

LIST (Lidar Surface Topography) is as one of a longer term missions recommended tasks by NASA, the main purpose of which is to achieve real high-resolution laser imaging mapping [1]. The LIST system uses at least 1000 laser beams for detection

(10 lasers), and each laser is divided into 100 beams. The laser repetition frequency is 10 kHz, and the energy of each beam is about 50 μJ ∼ 100 μJ [7].

In this paper, combining with the radar equation and single photon detection probability theory, the photon-counting Lidar performance indexes under different parameters is studied, and a feasible parameter suggestion of Lidar for satellite is put forward.

2 Theoretical Analysis

In the direct detection Lidar system, the number of signal photons detected from the diffuse target obeys the negative binomial distribution. In photon counting system of Lidar, the signal received by the detector is usually in the order of single photon. When the average number of photon detected is far less than the speckle degree of freedom of the receiving optical system, the Poisson distribution can be used to approximate the negative binomial distribution. Therefore, the Poisson distribution can be used to analyze the signal photoelectron produced by single photon detector, which can reflect the system characteristics more accurately.

According to the theory of Degnan [8], the probability of the signal in each measure frame is defined as follows.

$$P_{acq} = P(N_t \geq K) = 1 - e^{-N_t} \sum_{k=0}^{K-1} \frac{N_t^k}{k!} \tag{1}$$

where Nt is the sum of the mean signal and background counts in a measure frame, and the K is the frame count threshold.

Since the probability of noise detection also obey Poisson distribution, the false alarm probability of a single time unit is also as follows:

$$P_{false} = P(N_b \geq K) = 1 - e^{-N_b} \sum_{k=0}^{K-1} \frac{N_b^k}{k!} \tag{2}$$

where the Nb is the average number of noise photons in a single time unit. In order to distinguish signal photons and noise photons in a frame, N(k) is given by

$$N(K) = P_{acq} - P_{false} \tag{3}$$

where N(k) shows the difference between the detection probability of signal photons and noise photons.

For a given photon-counting Lidar system, the probability of the signal and false alarm probability are also related to the instrument contrast C, as shown in the following formula:

$$C = \frac{N_t}{N_b} = \frac{N_b + N_b}{N_b} \tag{4}$$

Figure 1 shows the relation between the N(k) and the number of photons in different C. It can be seen that with the improvement of instrument contrast C, the N(k) also increases, indicating that higher instrument contrast has higher discrimination for real photon events.
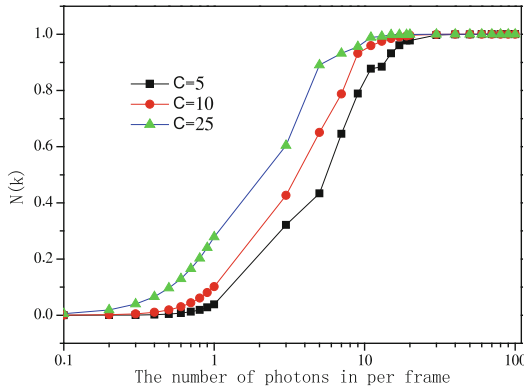

Fig. 1. Difference between the intra detection probability and the false alarm probability with the number of photons in per frame

3   Data Validation

3.1   Photon Number of Signal and Background Noise

When the measured object target is an area target, according to the classical altimeter equation, the mean number of signal photoelectrons per laser fire is given by [8]:

$$n_s = [\rho \cos \sigma T_0^2] \frac{\eta_q \eta_r E_t A_r}{\pi h \nu R^2} \qquad (5)$$

where ρ is the surface reflectivity, σ is the mean surface slope within the laser footprint, η_q is the detector quantum efficiency, η_r is the transmission efficiency of the receiver optics, E_t is the transmitted energy, A_r is the area of the receiver, $h\nu$ is the laser photon energy, R is the range to the surface.

Assuming the Lidar aperture of ~ 1 m, the surface slope $\sim 25°$, the typical surface reflectance of ~ 0.1, the height of orbit ~ 500 km, the emits energy of ~ 100 μJ, the number of returned photons is close to 1 photon.

Compared with 70 mJ of ICESat-1 satellite with full waveform ranging system, the energy of photon-counting Lidar is reduced by three orders of magnitude. Therefore, in the same size of Lidar aperture, the photon detection mode needs less energy of the laser, and it is possible to achieve hundreds beams or even thousands beams laser ranging.

In the actual flight process, the dynamic range of photon detection laser rangefinder needs to take into account the soil with low reflectivity and the ice with high reflectivity

Table 1. Summary of parameters used in photon-counting Lidar analysis

Characteristics	Value
Reflectance@532 nm, ρ	$0.05 \sim 0.6$
Surface slope, σ	$25°$
One-way transmission, T_0	70%
Detector quantum efficiency, η_q	20%
Receiver optical efficiency, η_r	40%
transmitted energy, E_t	150 uJ
Lidar aperture, r	1000 mm
Altitude, R	500 km
Solar spectral illuminance, N_λ^0	2 W/m²/nm
Spectral filter bandwidth, $\Delta\lambda$	50pm
Receiver field of view, θr	80 urad
Solar zenith angle, θs	$5°$

in order to be widely used. According to the parameters in Table 1, the average number of single pulse back-up photons of the on-board photon detection Lidar is about $0.71pe \sim 8.5pe$ within the range of surface reflectance $0.05 \sim 0.6$.

The noise sources of photon-counting Lidar are mainly solar background light noise caused by atmospheric scattering, background light noise caused by surface reflection and dark count noise of detector itself. According to the current device development level, the dark count noise of the detector is usually in the order of tens to thousands of Hertz, and the background noise is usually in the order of Mega-Hertz. Therefore, the noise is mainly caused by atmospheric backscattering and surface reflection. According to Degnan's theory [8], the noise is as follows.

$$n_s = [N_\lambda^0(\Delta\lambda)\Omega_r\tau_b][\frac{\eta_q\eta_r A_r}{\pi h\nu}][\rho T_0^{1+\sec\theta_s}\cos\psi + \frac{1 - T_0^{1+\sec\theta_s}}{4(1+\sec\theta_s)}] \qquad (6)$$

where N_λ is solar spectral illuminance, $\Delta\lambda$ is Spectral filter bandwidth, Ωr is the the receiver field of view (FOV) in steradians, τ_b is the duration of the range bin in vertical direction, θ_s is solar zenith angle.

From the above parameters, it can be calculated that the background noise intensity caused by atmosphere and surface is about 3×10^6 pe/s, which is equivalent to the typical noise rate of ICESat-2 [9].

3.2   Photon Number of Signal and Background Noise

For the photon counting Lidar, the average noise intensity is much greater than the signal intensity in the case of single pulse. Although the time, space and spectral

filtering methods are used in the system design to suppress the noise as much as possible, the high sensitivity of the detection system still trigger as detecting event due to the solar background light noise and surface reflection noise.

The background noise events are distributed randomly and evenly in the time range of a single detection, while the signal has a high probability in the target area. Although it is difficult to distinguish the signal and noise for a single detection, the event of signal and noise can be effectively identified by using the difference of the probability between noise event and signal event near the target area and combining with numerical statistics.

At present, there are many methods for laser point cloud data processing, which use the statistical characteristics of photon counting Lidar detection model to divide the sampling cell into multiple range grids. Because the detection probability of the target signal is much higher than that of the noise signal, the target signal can be extracted by using the high contrast statistical characteristics.

Figure 2 shows the relation between detection probability and threshold in different grid sizes of the ground surface. With the increase of grid size, the detection probability increases gradually under the same threshold of the photons.
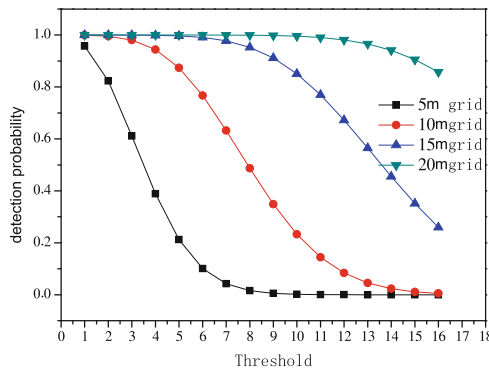

Fig. 2. Detection probability in different threshold of the photons (Reflectance 0.02, platform).

Figure 3 shows the relation between N(k) and threshold in different grid sizes. As can be seen from Fig. 3, the optimal detection threshold corresponding to different grid sizes is also different. Therefore, when the surface reflectance ($\sim$0.02) is low and the slope is relatively gentle, we can increase the grid size to obtain higher detection probability.
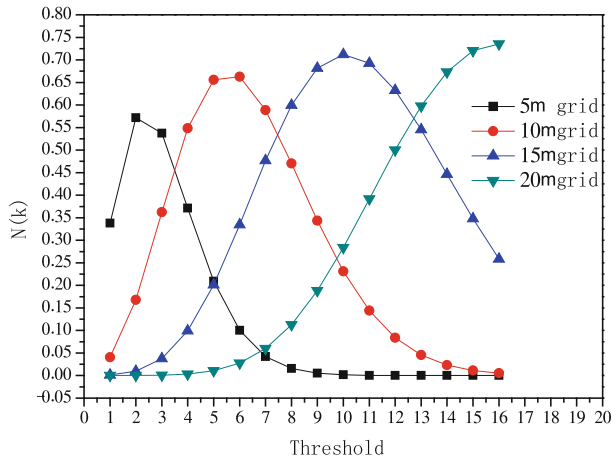
Fig. 3. Difference between the intra detection probability and the false alarm probability in different threshold (Reflectance 0.02, platform).

The application scene of the ranging Lidar is usually the ground surface, and the typical reflectivity of the surface is usually better than 0.1. In Fig. 4 and Fig. 5, the relationship between the detection probability,alert probability and the different threshold in different noise levels is analyzed. It can be seen that high noise rate will lead to high detection probability and the high false alarm probability. The key is how to distinguish the event of signal form noise.
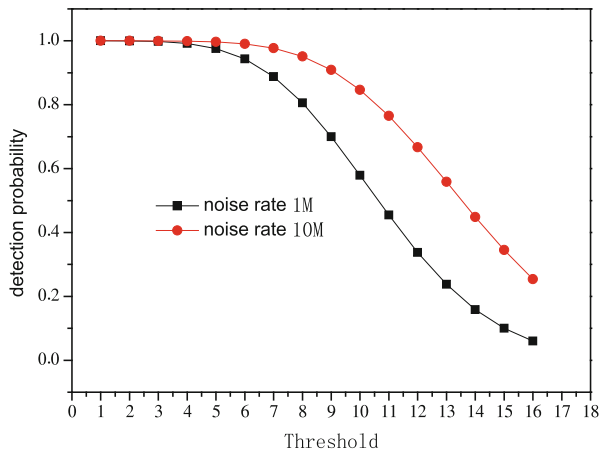

Fig. 4. Detection probability with different threshold in different noise rate.
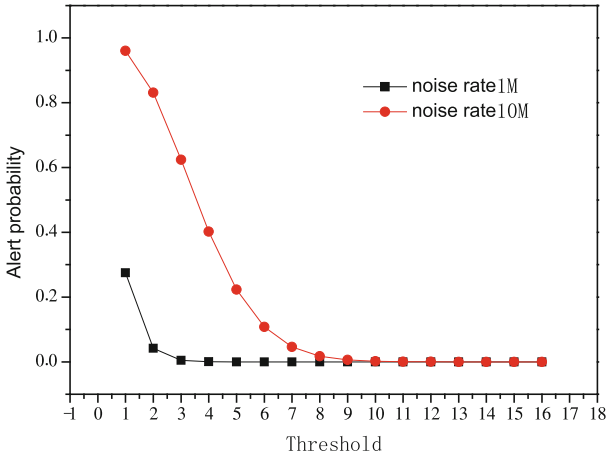
Fig. 5. Alert probability with different threshold in different noise rate.

Figure 6 shows the difference between the detection probability and the false alarm probability under different noise rate levels. In the case of 1 MHz noise rate, the detection probability of 99.78% can be achieved when the threshold of photons is 3pe; in the case of 10 MHz noise rate, the detection probability of 97.7% can be achieved when the threshold of photons is 7pe.
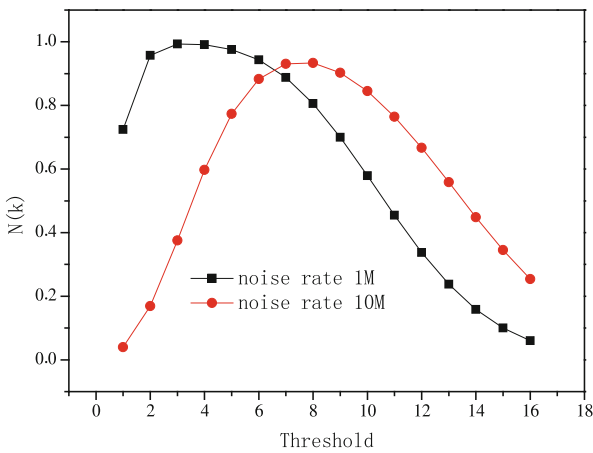

Fig. 6. Difference between the intra detection probability and the false alarm probability different threshold.

4   Conclusion

Under the given working conditions of photon-counting Lidar, the detection performance of photon counting Lidar is analyzed by using probability statistics method:

1) The contrast of the instrument has a great influence on the detection probability, and the lidar with high contrast has a high detection probability;
2) When the surface reflectance is relatively low and the slope is relatively gentle, higher detection probability can be obtained by increasing the surface grid size at the expense of surface measurement density;
3) Considering satellite and payload scale, a spaceborne Lidar with energy 100 μJ,and optical aperture 1m working in orbit of 500 km is an alternative.

References

1. Krainak, M.A., Abshire, J.B.: Laser transceivers for future NASA missions, laser technology for defense and security VIII. In: Proceedings of SPIE, vol. 8381, pp. 83810Y-1–83810Y-11 (2012)
2. Edwards, R., Sawruk, N.W.: ICESat-2 laser technology development, lidar remote sensing for environmental monitoring XIV. In: Proceedings of SPIE, vol. 8872, pp. 88720S-1–88720S-6 (2013)
3. Magruder, L.A., Brunt, K.M.: Performance analysis of airborne photon-counting lidar data in preparation for the ICESat-2 mission. IEEE Trans. Geosci. Remote Sens. **56**(5), 2911–2918 (2018)
4. Brown, M.E., Arias, S.D.: Applications for ICESat-2 data. IEEE Geosci. Remote Sens. Mag. **4**(4), 24–37 (2016). 0274–6638
5. Zhu, X.X., Nie S.: The performance of ICESat-2's strong and weak beams in estimating ground elevation and forest height. In: IEEE International Geoscience and Remote Sensing Symposium, pp. 6073–6076 (2020). 978-1-7281-6374-1
6. Anthony, M., Thomas, N.: ICESat-2 mission overview and early performance. In: Proceedings of SPIE, vol. 1115, pp. 111510C-1–111510C-10 (2019)
7. Yu, A.W., Krainak, M.A.: Multi-beam Laser Altimeter System Simulator for the Lidar Surface Topography (LIST) Mission, CLEO Technical Digest, OSA (2012)
8. Degnan, J.J.: Photon-counting multikilohertz microlaser altimeters for airborne and spaceborne topographic measurements. J. Geodyn. **34**, 503–549 (2002)
9. Zhang, J.S., Kerekes, J.: An adaptive density-based model for extracting surface returns from photon-counting laser altimeter data. IEEE Geosci. Remote Sens. Lett. **12**(4), 726–730 (2015)